Chemical Science

ROYAL SOCIETY OF CHEMISTRY

EDGE ARTICLE

View Article Online
View Journal | View Issue

Cite this: *Chem. Sci.*, 2025, **16**, 3580

All publication charges for this article have been paid for by the Royal Society of Chemistry

Received 9th January 2025
Accepted 19th January 2025

DOI: 10.1039/d5sc00190k

rsc.li/chemical-science

Modular assembly of amines and diborons with photocatalysis enabled halogen atom transfer of organohalides for C(sp^3)–C(sp^3) bond formation†

Rong-Bin Liang,‡[a] Ting-Ting Miao,‡[a] Xiang-Rui Li,[a] Jia-Bo Huang,[a] Shao-Fei Ni,*[a] Sanliang Li,[a] Qing-Xiao Tong[a] and Jian-Ji Zhong*[ab]

In the past few years, the direct activation of organohalides by ligated boryl radicals has emerged as a potential synthetic tool for cross-coupling reactions. In most existing methods, ligated boryl radicals are accessed from NHC-boranes or amine-boranes. In this work, we report a new photocatalytic platform by modular assembly of readily available amines and diboron esters to access a library of ligated boryl radicals for reaction screening, thus enabling the cross-coupling of organohalides and alkenes including both activated and unactivated ones for C(sp^3)–C(sp^3) bond formation by using the assembly of DABCO **A1** and B_2Nep_2 **B1**. The strategy features operational simplicity, mild conditions and good functional group tolerance. A range of organohalides including activated alkyl chlorides, alkyl bromides (1°, 2° and 3° C–Br) as well as aromatic bromides are applicable in the strategy. Experimental and computational studies rationalize the proposed mechanism.

Introduction

Halogen atom transfer (XAT) of organohalides to the corresponding carbon-centered radicals for subsequent transformations is a powerful synthetic strategy in organic synthesis.[1,2] Historically, tin-containing reagents as efficient halogen abstractors have made great contributions to this field.[3,4] However, the safety and selectivity concerns about tin-containing reagents drive an ever-increasing interest in seeking alternatives.[5] In the last few decades, photoredox catalysis[6–17] has emerged as a green and efficient platform for the activation of organohalides *via* XAT by silyl radicals[18–23] and α-aminoalkyl radicals.[24–27] In recent years, photocatalytically generated ligated boryl radicals (LBRs), which exhibit a comparable performance in halogen atom abstraction, are found to be a promising alternative. Nevertheless, compared with silyl radicals and α-aminoalkyl radicals, ligated boryl radicals[28–48] mediated XAT for cross-couplings is still in its infancy and has been less explored. To the best of our knowledge, only several successful examples have so far been reported. For example, as illustrated in Scheme 1a, Wu[49] and Leonori,[50,51] respectively, reported that tertiary amine-borane **LB1** was able to activate the C–Cl bond of Freon-22 ($ClCF_2H$) or the C–I/Br bond of alkyl halides for alkylation of alkenes or alkynes under

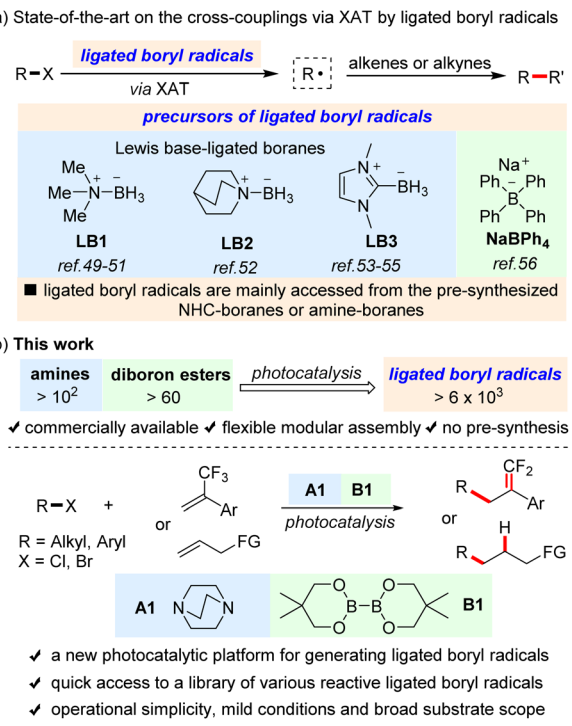

Scheme 1 (a) State-of-the-art of the cross-couplings *via* XAT by ligated boryl radicals. (b) This work.

[a]*College of Chemistry and Chemical Engineering, Key (Guangdong-Hong Kong Joint) Laboratory for Preparation and Application of Ordered Structural Materials of Guangdong Province, Shantou University, Shantou 515063, P. R. China. E-mail: jjzhong@stu.edu.cn*

[b]*Chemistry and Chemical Engineering Guangdong Laboratory, Shantou 515063, P. R. China*

† Electronic supplementary information (ESI) available. See DOI: https://doi.org/10.1039/d5sc00190k

‡ These two authors contributed equally.

photocatalysis. Subsequently, Wu disclosed that tertiary amine-borane **LB2** with photocatalysis could activate the C–Cl bond of $ClCF_2R$ for difluoromethylation of alkenes.[52] In addition, the groups of Noël,[53] Capaldo,[54] and Fan,[55] respectively, reported that N-heterocyclic carbene–borane **LB3** with photocatalysis could activate the C–I bond of alkyl iodides to initiate Giese-type reactions. Very recently, Sharma[56] reported that, after photocatalytic single-electron oxidation, sodium tetraphenylborate ($NaBPh_4$) could generate a reactive boryl radical to enable hydroalkylation of styrenes with alkyl iodides or bromides. Although such progress has been made, the ligated boryl radicals in the existing methods are mainly accessed from pre-synthesized NHC-boranes or amine-boranes, and the boryl-radical precursors are limited to a few Lewis base-ligated boranes, which restricts the application of ligated boryl radical-mediated XAT for cross-coupling reactions. Therefore, the development of new methodologies to generate various reactive ligated boryl radicals will be interesting and highly desirable. In this work, we report a new photocatalytic platform by modular assembly of commercially available amines and diboron esters, which provides a simple and convenient approach to access a library of various reactive ligated boryl radicals for reaction screening, thus enabling the cross-coupling of organohalides and alkenes including both the activated and unactivated ones for $C(sp^3)$–$C(sp^3)$ bond formation by using the assembly of DABCO **A1** and B_2Nep_2 **B1** under photocatalysis.

Results and discussion

Dichloromethane (DCM), one of the most ubiquitous solvents, is widely used in chemical research and industry. It would be a desirable C1 synthon if the ligated boryl radical could selectively activate the C–Cl bond. However, due to its inertness and low reactivity, the activation of C–Cl bond in dichloromethane for organic transformations is still rather limited.[57] To this end, we commenced our investigations by evaluating the activation of dichloromethane using various reactive ligated boryl

Table 1 Optimization of the reaction parameters[a]

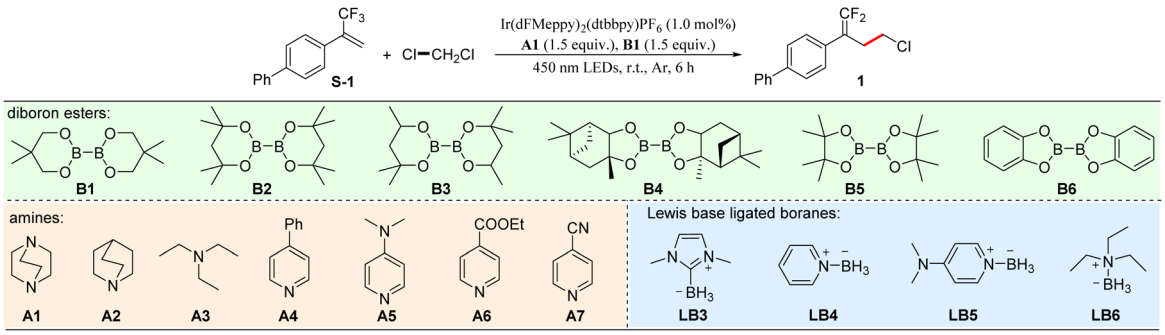

Entry	Variations from the standard conditions	1[b] (%)
1	None	91
2	4CzIPN instead of $Ir(dFMeppy)_2(dtbbpy)PF_6$	72
3	Mes-Acr-$Me^+ClO_4^-$ instead of $Ir(dFMeppy)_2(dtbbpy)PF_6$	Trace
4	$Ru(bpy)_3(PF_6)_2$ instead of $Ir(dFMeppy)_2(dtbbpy)PF_6$	Trace
5	$Ir(ppy)_3$ instead of $Ir(dFMeppy)_2(dtbbpy)PF_6$	Trace
6	**B2** instead of **B1**	72
7	**B3** instead of **B1**	83
8	**B4** instead of **B1**	67
9	**B5** instead of **B1**	76
10	**B6** instead of **B1**	Trace
11	**A2** instead of **A1**	24
12	**A3** instead of **A1**	12
13	**A4** instead of **A1**	56
14	**A5** instead of **A1**	41
15	**A6** instead of **A1**	14
16	**A7** instead of **A1**	NR
17	**LB3** instead of **A1**&**B1**	29
18	**LB4** instead of **A1**&**B1**	36
19	**LB5** instead of **A1**&**B1**	27
20	**LB6** instead of **A1**&**B1**	Trace
21	Without $Ir(dFMeppy)_2(dtbbpy)PF_6$, light, **A1**, or **B1**	NR

[a] Standard conditions: **S-1** (0.2 mmol), photocatalyst (1.0 mol%), **A1** (0.3 mmol), **B1** (0.3 mmol), CH_2Cl_2 (2.0 mL), r.t., Ar atmosphere, and 450 nm LED irradiation for 6 h. [b] Isolated yields.

radicals, which were *in situ* generated from the platform of modular assembly of commercially available amines and diboron esters under photocatalysis. After extensive screenings, we were delighted to find that when α-trifluoromethyl arylalkene **S-1** was selected as the substrate, the assembly of tertiary amine **A1** and diboron ester **B1** with $Ir(dFMeppy)_2(dtbbpy)PF_6$ as a photocatalyst could successfully furnish the desired chloromethylation product, the *gem*-difluoroalkene **1**, in 91% yield with excellent chemo-selectivity at room temperature under 450 nm LED irradiation for 6 h (Table 1, entry 1). Herein, dichloromethane served not only as a raw material, but also as a solvent. Replacing the photocatalyst with 4CzIPN resulted in a decreased yield of 72% (entry 2). Trace amount of the desired product was observed when other photocatalysts such as Mes-Acr-$Me^+ClO_4^-$, $Ru(bpy)_3(PF_6)_2$, or $Ir(ppy)_3$ was used (entries 3–5). Moreover, other assemblies of amines and diboron esters were examined (entries 6–16), and the assembly of **A1** and **B1** proved to be the best. Additionally, several NHC-boranes or amine-boranes, which are commonly used precursors of ligated boryl radicals under photocatalysis, were tested, however, they could not accelerate this transformation in a satisfactory yield (entries 17–20), demonstrating the advantages of this flexible platform. Finally, no desired product was detected when the reaction took place in the absence of the photocatalyst, light, **A1** or **B1**, indicating the essential role of all these parameters (entry 21).

Table 2 Substrate scope of the C–Cl activation reaction[a,b]

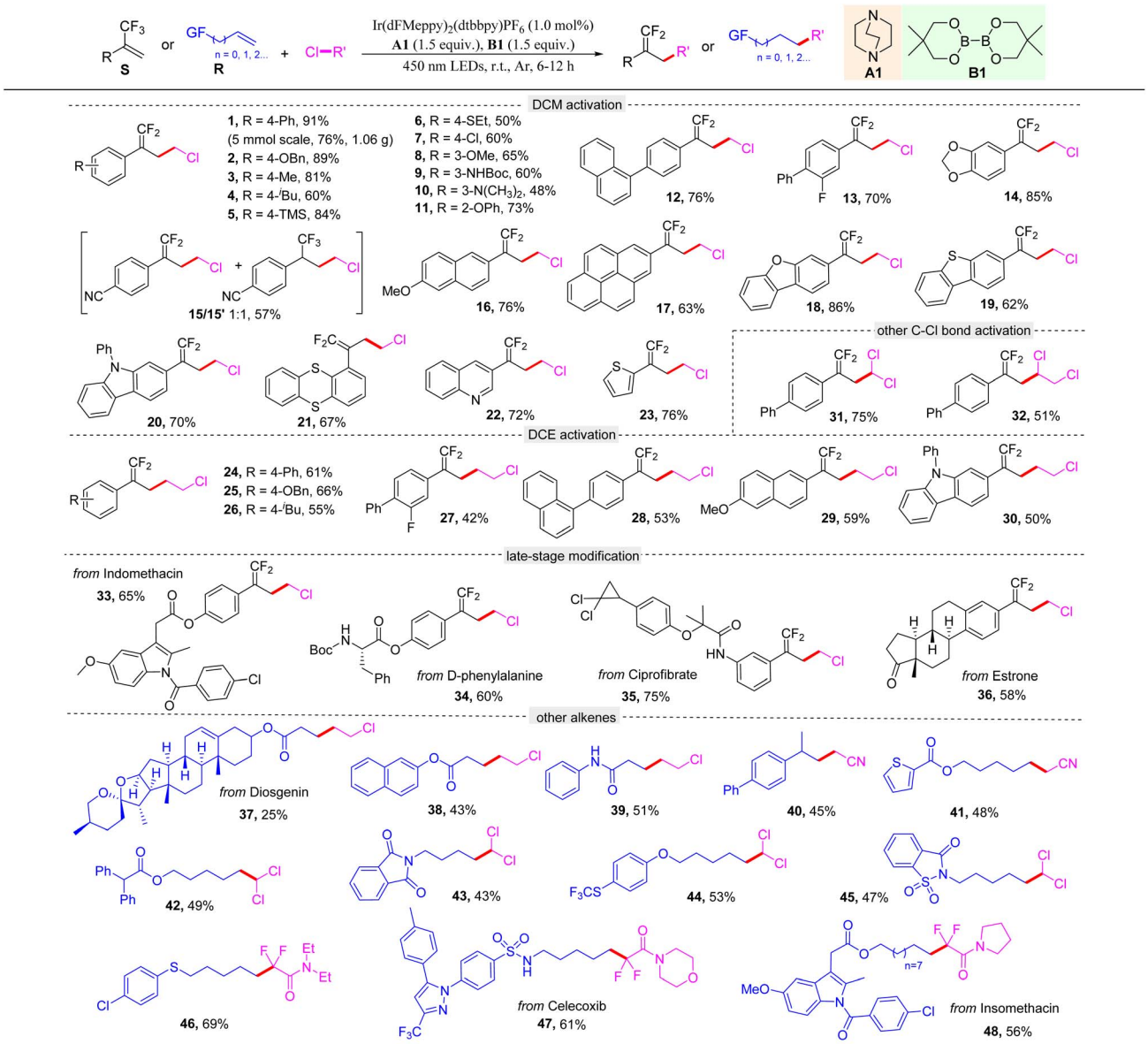

[a] Standard conditions: **S** or **R** (0.2 mmol), photocatalyst (1.0 mol%), **A1** (0.3 mmol), **B1** (0.3 mmol), RCl (2.0 mL), r.t., Ar, and 450 nm LED irradiation for 6–12 h. [b] Isolated yields.

To verify the generality of this photocatalytic protocol for the C–Cl activation reaction, we first evaluated the scope of alkenes (Table 2). To our delight, various α-trifluoromethyl arylalkenes bearing different functional groups, regardless of electron-donating or electron-withdrawing groups, on the aromatic ring were all well tolerated, giving the corresponding chloromethylation *gem*-difluoroalkenes **1–14** in good to excellent yields. Notably, when the *para*-position of the aromatic ring was substituted by a strong electron-withdrawing group such as the cyano group, besides the desired product **15**, the hydrochloromethylation of alkene was competitive to afford a byproduct **15′**, probably due to the fact that delocalization of the electron density into the electron-poor ring slows down the fluoride elimination. Trifluoromethyl alkenes possessing different aromatic scaffolds, including naphthalene (**16**), pyrene (**17**), dibenzofuran (**18**), dibenzothiophene (**19**), carbazole (**20**), thianthrene (**21**), quinoline (**22**), and thiophene (**23**) moieties, were all compatible with the reaction to deliver the corresponding products in good yields. With respect to the C–Cl precursor, the protocol could also activate the C–Cl bond of another commonly used industrial feedstock dichloroethane (DCE) to give the corresponding products **24–30** in moderate to good yields. Additionally, the C–Cl bonds of chloroform and trichloroethane could also be activated to furnish **31** and **32** in 75% and 51% yields, respectively. To illustrate the practicability of this protocol, a gram-scale reaction was conducted, and the desired product **1** was obtained in 76% yield. Moreover, the mild conditions and excellent functional group tolerance inspired us to explore its application to late-stage modification of complex molecules. To our delight, the trifluoromethyl alkenes derived from indomethacin, D-phenylalanine, ciprofibrate, and estrone successfully afforded the corresponding products **33–36** in satisfactory yields. Furthermore, inspired by the case of **15**, we envisioned that the photocatalytic protocol was probably able to enable a hydroalkylation reaction. Indeed, when we employed this protocol to activate the C–Cl bonds of DCE, $ClCH_2CN$, chloroform, and various $ClCF_2R$, the corresponding carbon-centered radicals could smoothly react with a range of alkenes including various activated and unactivated ones to give the corresponding hydroalkylation products **37–48** in moderate yields.

Encouraged by the above results, we wondered whether this protocol would be able to activate the C–Br bond of organic bromides. Therefore, a broad set of organic bromides reacting with α-trifluoromethyl arylalkene **S-2** were examined. It should be noted that herein 5.0 equivalent of organic bromides was used, and acetonitrile was selected as a solvent. As shown in Table 3, primary alkyl bromides bearing various functional groups, including different chain length alkyl (**49–52**), ether (**53**), *tert*-butyl carbamate (**54**), free hydroxyl (**55–57**), furan (**58**), ester (**59**), and vinyl (**60**, **61**) groups, were all well tolerated to give the corresponding alkylation products in moderate to good

Table 3 Substrate scope of the C–Br activation reaction[a,b]

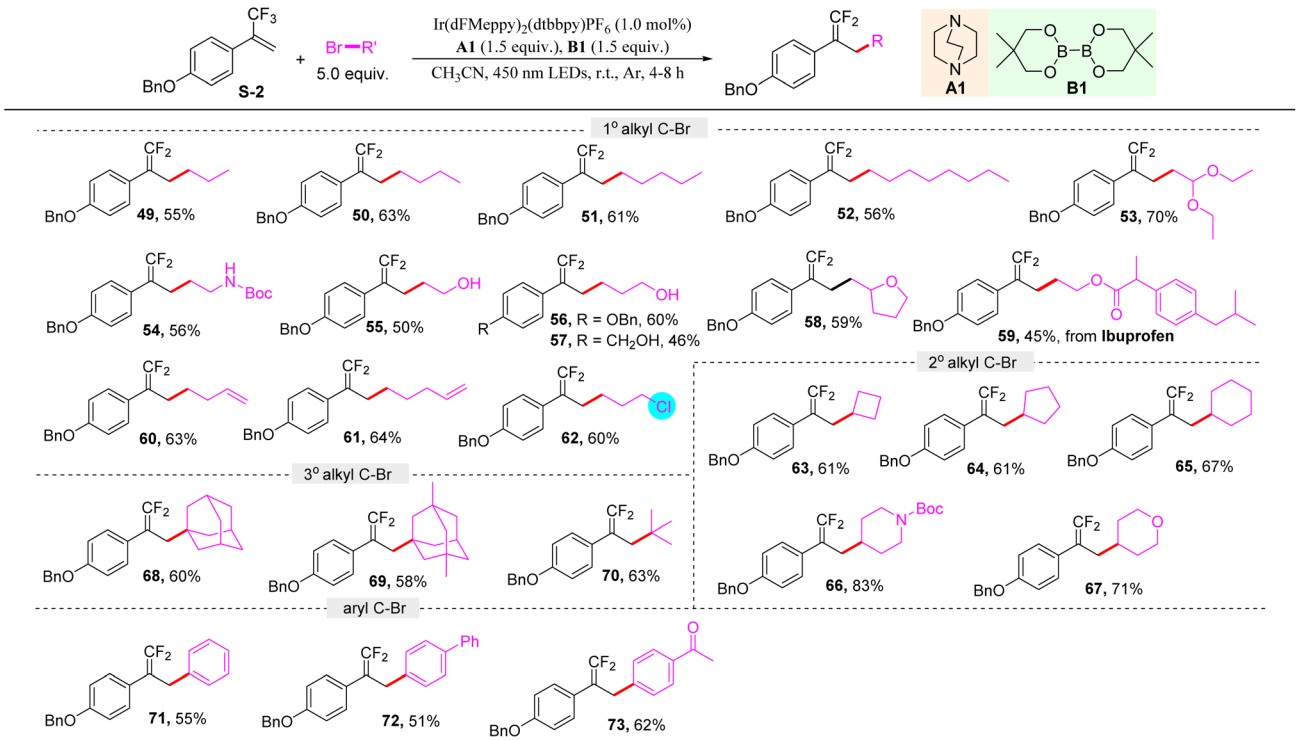

[a] Standard conditions: **S-2** (0.2 mmol), photocatalyst (1.0 mol%), **A1** (0.3 mmol), **B1** (0.3 mmol), RBr (5.0 equiv.), CH_3CN (3.0 mL), r.t., Ar, and 450 nm LED irradiation for 4–8 h. [b] Isolated yields.

yields. Notably, when 1-bromo-3-chloropropane was used in this protocol, the C–Br bond was selectively activated to access **62** in 60% yield, and the C–Cl bond remained intact. Secondary alkyl bromides such as cyclobutyl (**63**), cyclopentyl (**64**), cyclohexyl (**65**), piperidyl (**66**), and pyranyl (**67**) bromides were all suitable substrates. Furthermore, tertiary alkyl bromides were also found to be amenable to deliver the products **68–70** in good yields. Moreover, the C(sp^2)–Br bond of aromatic bromides could also be activated to realize this transformation with high efficiency (**71–73**), demonstrating the excellent ability of ligated boryl radicals from this protocol for C–Br bond activation.

A series of experimental studies were carried out to gain insights into the reaction mechanism (Scheme 2). When a radical scavenger 2,2,6,6-tetramethyl-1-piperidinyloxy (TEMPO) was added into the model reaction under standard conditions, formation of the desired product **1** was completely inhibited, and the adduct TEMPO-CH_2Cl was detected by high resolution mass spectrometry (HRMS) (Scheme 2a). In addition, the radical-clock experiment with cyclopropylmethyl bromide under standard conditions afforded the ring-opening product **60** in 53% yield (Scheme 2b). These results suggested that the reaction proceeded *via* a radical pathway. For the hydroalkylation reaction, to confirm the hydrogen source of the products, the reaction of **R-39** with cyclohexyl bromide under standard conditions using d_3-CH_3CN was conducted, just a small amount of deuterium atom was incorporated into the product **74**. Moreover, addition of 30 equivalent of deuterium oxide to the reaction resulted in 83% deuterium incorporation, suggesting that the hydrogen source of the product is the H_2O in the solvent (Scheme 2c). Furthermore, Stern–Volmer quenching experiments were conducted as shown in Scheme 2d(1). The results revealed that the excited-state photocatalyst could not be quenched by trifluoromethyl alkene **S-1**, **B1**, or dichloromethane, while it could be effectively quenched by the assembly of **A1** and **B1** or **A1** alone, and their quenching efficiencies are comparable. Additionally, cyclic voltammetry experiments showed that the oxidation potential of the assembly of **A1** and **B1** is almost the same as that of **A1** at about +0.83 V *vs.* SCE (Scheme 2d(2)). These results indicated that the single electron transfer between the photocatalyst and the assembly of **A1** and **B1** is feasible, and it is actually initiated by the photocatalytic oxidation of **A1**. Moreover, a series of ^{11}B NMR monitoring experiments were carried out. As shown in Scheme 2e, in spectrum V of the crude mixture after the reaction was complete, a new species with a chemical shift of 18.14 ppm was observed, which was assigned to the signal of HO-Bnep.[58] And the generation of HO-Bnep could be further detected by HRMS. In spectrum I and II, a chemical shift difference of 0.52 ppm was observed, revealing a weak coordination between **A1** and **B1**. Additionally, in spectrum III and IV, the signal of HO-Bnep was still observed even without **A1**. The above results indicated that besides the photocatalyst and **A1**, H_2O in the solvent probably participated in accelerating the B–B bond cleavage of **B1** to generate the reactive ligated boryl radical. Therefore, a control reaction under rigorous exclusion of H_2O was conducted, the yield was sharply decreased to 43%, further confirming that H_2O could promote this transformation (Scheme 2f). Note that an amino radical transfer (ART) mechanism was reported to enable the generation of ligated boryl radicals from alkyl boronic esters,[59] while primary or secondary alkylamines are typically required in those cases. In this work, tertiary amines (**A1–A3**) or pyridines (**A4–A6**) were used. Thus, a mechanism through the single electron transfer between the photocatalyst and the assembly of **A1** and **B1** rather than the ART mechanism is more reasonable in this protocol.

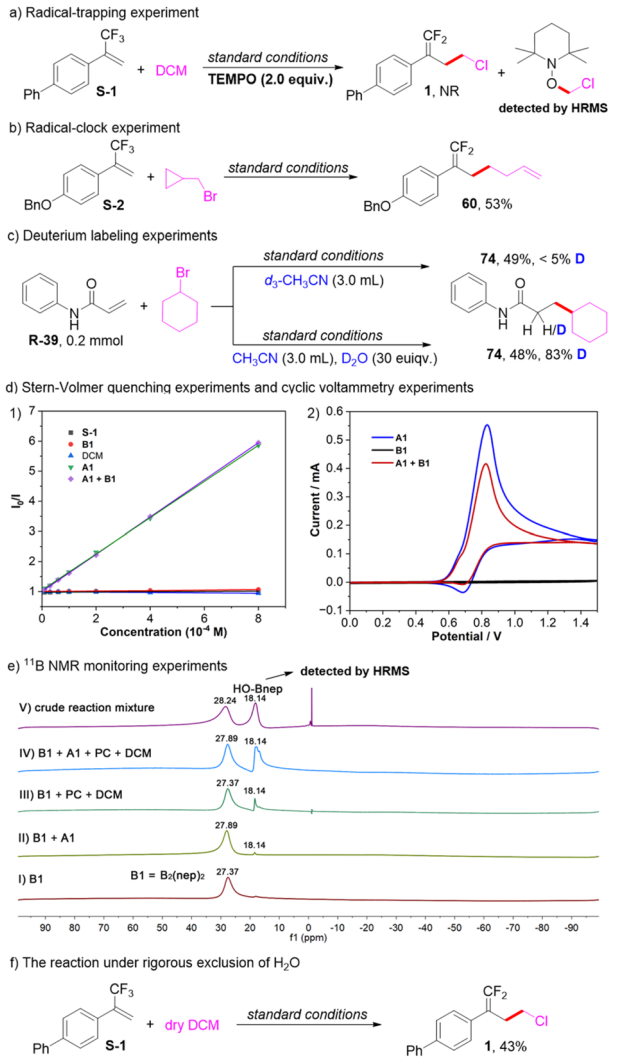

Scheme 2 (a) Radical-trapping experiment. (b) Radical-clock experiment. (c) Deuterium labeling experiments. (d) Luminescence quenching experiments and cyclic voltammetry experiments. (e) ^{11}B NMR monitoring experiments. (f) The reaction under rigorous exclusion of H_2O.

Based on the above experimental results, computational studies were carried out for further understanding of the generation of ligated boryl radicals (Scheme 3). First, the weak coordination of tertiary amine **A1** to one boron atom of **B1** produced the intermediate **INT-1**, with a slightly activated B–B bond elongated from 1.713 Å to 1.743 Å, which is in accordance with the observation in the ^{11}B NMR spectrum I and II (Scheme 2e). Then, **INT-1** could be stabilized by one molecule of water to form a more stable intermediate **INT-2**, with two O–H···O

hydrogen bonding interactions ($b1$ = 1.835 Å, $b2$ = 2.131 Å) observed. Frontier molecular orbital analysis indicated that the HOMO orbital of **B1** could be activated with the coordination of amine and water, which was elevated from −7.32 eV (**B1**) to −5.20 eV (**INT-1**) and −5.51 eV (**INT-2**), respectively. Additionally, orbital diagrams showed that the HOMO orbital of **B1** was mainly assigned to the two boron atoms. In comparison, the nitrogen atom in the tertiary amine made some contribution to the HOMO orbital of **INT-1** and **INT-2**, indicating that the tertiary amine played a role in the activation of the B–B bond. The cleavage of the B–B bond happened with the aid of the single electron transfer (SET) process by the photocatalyst, producing a radical cation species **INT-3** with an energy difference of 7.5 kcal mol^{-1} in terms of Gibbs free energy. The B–B bond in **INT-2** was calculated to be 1.746 Å, and was totally cleaved to 2.164 Å in **INT-3**. Relaxed potential energy scan showed that the B–B bond cleavage process was barrierless (see more details in the ESI, Fig. S3a†). Then, the deprotonation process released the energy of 29.2 kcal mol^{-1} with the aid of tertiary amine **A1** to form **INT-4**. Structural analysis showed that the bond length of the O–H bond increased from 1.032 Å in **INT-3** to 1.632 Å in **INT-4**, indicating that the proton was transferred from HO-Bneop to the tertiary amine, which was also confirmed to be barrierless (see more details in the ESI, Fig. S3b†). Finally, **INT-4** may have readily dissociated into three parts, HO-Bneop, protonated tertiary amine **HA1**$^+$ and tertiary amine-ligated boryl radical **BN**. Though experimental and computational studies provide us a rational pathway, the exact nature of the generation of ligated boryl radicals is still unclear due to the complexity of this photocatalytic system, more detailed investigations need to be conducted in the future.

Based on the above experimental and computational results, a plausible mechanism is proposed as shown in Scheme 4. With the aid of tertiary amine **A1** and H_2O, the activation of the B–B bond of diboron ester **B1** through single-electron transfer by the excited-state photocatalyst PC*, which is a feasible process supported by luminescence quenching experiments and cyclic voltammetry experiments, generates the reduced photocatalyst PC$^-$ and tertiary amine-ligated boryl radical **BN**. Then, **BN** undergoes a facile halogen atom transfer with organohalides to result in the generation of the corresponding alkyl radical R$^\bullet$, which can be trapped by alkenes *via* intermolecular radical addition to furnish a new alkyl radical **I-1**. Subsequently, single-electron transfer from PC$^-$ to **I-1** regenerates the photocatalytic cycle and produces a carbanion intermediate **I-2**. In the case of the trifluoromethyl alkene substrate, the following defluorination of **I-2** leads to the alkylation product *gem*-difluoroalkenes. In the case of the unactivated alkenes, subsequent protonation of **I-2** results in the final hydroalkylation products. It should be noted that in previous reports,[60–63] ligated boryl radicals were able to act as a highly reducing agent to activate aryl or alkyl halides *via* single electron transfer. In this work, considering the fact that the reduction potential of dichloromethane is too high, halogen atom transfer is believed to be the actual process to activate the C–X bond of organohalides. However, the activation *via* the SET mechanism could not be completely excluded.

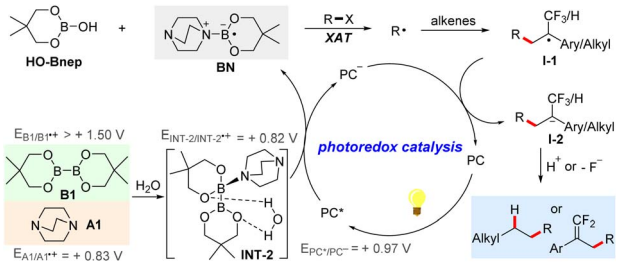

Scheme 4 Plausible mechanism.

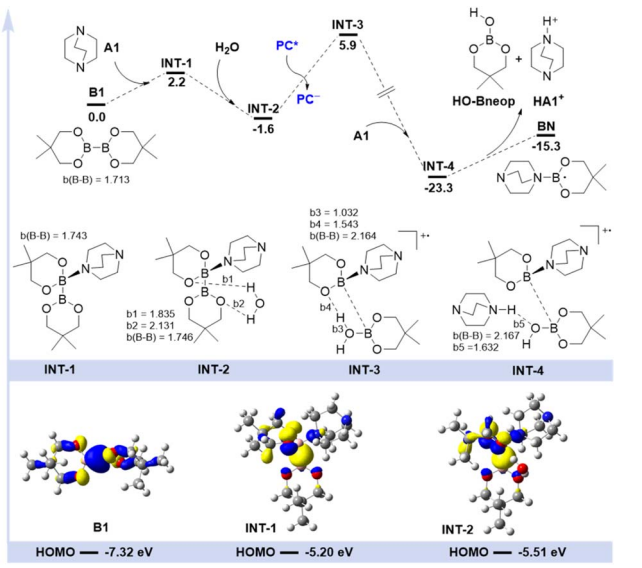

Scheme 3 DFT calculated potential energy surface and frontier molecular orbital analysis for the ligated boryl radical formation process in kcal mol^{-1}.

Conclusions

In summary, a new photocatalytic platform has been established to generate ligated boryl radicals. By flexible modular assembly of readily available amines and diboron esters, we can quickly access a library of various reactive ligated boryl radicals for reaction screening. Therefore, by employing the assembly of DABCO **A1** and B_2Nep_2 **B1**, the C–Cl/Br bond of organohalides could be effectively activated *via* a halogen atom transfer process, thus enabling the cross-coupling of organohalides with alkenes including activated and unactivated ones for C(sp^3)–C(sp^3) bond formation under photocatalysis. Experimental and computational studies rationalize that the ligated boryl radical is generated through the activation of the B–B bond of diboron ester *via* photoinduced single electron transfer with the aid of amine and H_2O. Such a protocol features mild conditions, good functional group tolerance and broad substrate scope. Scale-up synthesis and late-stage modification of structurally complex molecules demonstrate the practicability. Further application of this photocatalytic platform for ligated boryl radical-mediated organic transformations is ongoing in our laboratory.

Data availability

The data supporting this article have been included as part of the ESI.†

Author contributions

The manuscript was written through contributions of all authors. All authors have given approval to the final version of the manuscript. R. B. L., T. T. M., and X. R. L. designed and performed the experiments. J. B. H. and S. F. N. performed the density functional theory calculations. S. L. and Q. X. T. participated in the data discussion. J. J. Z. directed the project and wrote the manuscript.

Conflicts of interest

There are no conflicts to declare.

Acknowledgements

The authors gratefully acknowledge the financial support from the National Natural Science Foundation of China (22171177), the Guangdong-Hong Kong Joint Laboratory for Preparation and Application of Ordered Structural Materials of Guangdong Province (2023B1212120011), the Guangdong Basic and Applied Basic Research Foundation (2023A1515110791), the Chemistry and Chemical Engineering Guangdong Laboratory (2312002), and the Guangdong Major Project of Basic and Applied Basic Research (2019B030302009).

Notes and references

1 F. Juliá, T. Constantin and D. Leonori, *Chem. Rev.*, 2022, **122**, 2292–2352.
2 C.-L. Ji, X. Zhai, Q.-Y. Fang, C. Zhu, J. Han and J. Xie, *Chem. Soc. Rev.*, 2023, **52**, 6120–6138.
3 H. G. Kuivila and L. W. Menapace, *J. Org. Chem.*, 1963, **28**, 2165–2167.
4 S. Crespi and M. Fagnoni, *Chem. Rev.*, 2020, **120**, 9790–9833.
5 E. Le Grognec, J.-M. Chrétien, F. Zammattio and J.-P. Quintard, *Chem. Rev.*, 2015, **115**, 10207–10260.
6 K. Zeitler, *Angew. Chem., Int. Ed.*, 2009, **48**, 9785–9789.
7 T. P. Yoon, M. A. Ischay and J. Du, *Nat. Chem.*, 2010, **2**, 527–532.
8 J. M. Narayanam and C. R. Stephenson, *Chem. Soc. Rev.*, 2011, **40**, 102–113.
9 L. Shi and W. Xia, *Chem. Soc. Rev.*, 2012, **41**, 7687–7697.
10 C. K. Prier, D. A. Rankic and D. W. C. MacMillan, *Chem. Rev.*, 2013, **113**, 5322–5363.
11 D. A. Nicewicz and T. M. Nguyen, *ACS Catal.*, 2014, **4**, 355–360.
12 D. C. Fabry and M. Rueping, *Acc. Chem. Res.*, 2016, **49**, 1969–1979.
13 I. Ghosh, L. Marzo, A. Das, R. Shaikh and B. König, *Acc. Chem. Res.*, 2016, **49**, 1566–1577.
14 Q. Liu and L.-Z. Wu, *Natl. Sci. Rev.*, 2017, **4**, 359–380.
15 Y. Chen, L.-Q. Lu, D.-G. Yu, C.-J. Zhu and W.-J. Xiao, *Sci. China:Chem.*, 2018, **62**, 24–57.
16 X. Y. Yu, Q. Q. Zhao, J. Chen, W. J. Xiao and J. R. Chen, *Acc. Chem. Res.*, 2020, **53**, 1066–1083.
17 X. Y. Yu, J. R. Chen and W. J. Xiao, *Chem. Rev.*, 2021, **121**, 506–561.
18 P. Zhang, C. C. Le and D. W. C. MacMillan, *J. Am. Chem. Soc.*, 2016, **138**, 8084–8087.
19 A. ElMarrouni, C. B. Ritts and J. Balsells, *Chem. Sci.*, 2018, **9**, 6639–6646.
20 X. Yu, M. Lübbesmeyer and A. Studer, *Angew. Chem., Int. Ed.*, 2021, **60**, 675–679.
21 S. Mistry, R. Kumar, A. Lister and M. J. Gaunt, *Chem. Sci.*, 2022, **13**, 13241–13247.
22 A. Luridiana, D. Mazzarella, L. Capaldo, J. A. Rincón, P. García-Losada, C. Mateos, M. O. Frederick, M. Nuño, W. Jan Buma and T. Noël, *ACS Catal.*, 2022, **12**, 11216–11225.
23 G. H. Lovett, S. Chen, X.-S. Xue, K. N. Houk and D. W. C. MacMillan, *J. Am. Chem. Soc.*, 2019, **141**, 20031–20036.
24 T. Constantin, M. Zanini, A. Regni, N. S. Sheikh, F. Juliá and D. Leonori, *Science*, 2020, **367**, 1021–1026.
25 X.-S. Zhou, D.-M. Yan and J.-R. Chen, *Chem*, 2020, **6**, 823–825.
26 V. S. Kostromitin, A. O. Sorokin, V. V. Levin and A. D. Dilman, *Chem. Sci.*, 2023, **14**, 3229–3234.
27 F. Yue, J. Dong, Y. Liu and Q. Wang, *Org. Lett.*, 2021, **23**, 7306–7310.
28 T. Taniguchi, *Chem. Soc. Rev.*, 2021, **50**, 8995–9021.
29 L. Capaldo, T. Noël and D. Ravelli, *Chem Catal.*, 2022, **2**, 957–966.
30 T.-Y. Peng, F.-L. Zhang and Y.-F. Wang, *Acc. Chem. Res.*, 2023, **56**, 169–186.
31 J. A. Baban and B. P. Roberts, *J. Chem. Soc., Chem. Commun.*, 1983, 1224–1226.
32 S.-H. Ueng, A. Solovyev, X. Yuan, S. J. Geib, L. Fensterbank, E. Lacôte, M. Malacria, M. Newcomb, J. C. Walton and D. P. Curran, *J. Am. Chem. Soc.*, 2009, **131**, 11256–11262.
33 D. P. Curran, A. Solovyev, M. Makhlouf Brahmi, L. Fensterbank, M. Malacria and E. Lacôte, *Angew. Chem., Int. Ed.*, 2011, **50**, 10294–10317.
34 X. Pan, E. Lacôte, J. Lalevée and D. P. Curran, *J. Am. Chem. Soc.*, 2012, **134**, 5669–5674.
35 T. Kawamoto, S. J. Geib and D. P. Curran, *J. Am. Chem. Soc.*, 2015, **137**, 8617–8622.
36 G. Duret, R. Quinlan, P. Bisseret and N. Blanchard, *Chem. Sci.*, 2015, **6**, 5366–5382.
37 G. Wang, H. Zhang, J. Zhao, W. Li, J. Cao, C. Zhu and S. Li, *Angew. Chem., Int. Ed.*, 2016, **55**, 5985–5989.
38 A. Fawcett, J. Pradeilles, Y. Wang, T. Mutsuga, E. L. Myers and V. K. Aggarwal, *Science*, 2017, **357**, 283–286.
39 V. I. Supranovich, V. V. Levin, M. I. Struchkova, A. A. Korlyukov and A. D. Dilman, *Org. Lett.*, 2017, **19**, 3215–3218.
40 L. Zhang and L. Jiao, *J. Am. Chem. Soc.*, 2017, **139**, 607–610.

41 Y.-J. Yu, F.-L. Zhang, T.-Y. Peng, C.-L. Wang, J. Cheng, C. Chen, K. N. Houk and Y.-F. Wang, *Science*, 2021, **371**, 1232–1240.
42 Z. Ding, Z. Liu, Z. Wang, T. Yu, M. Xu, J. Wen, K. Yang, H. Zhang, L. Xu and P. Li, *J. Am. Chem. Soc.*, 2022, **144**, 8870–8882.
43 L. Kuehn, L. Zapf, L. Werner, M. Stang, S. Würtemberger-Pietsch, I. Krummenacher, H. Braunschweig, E. Lacôte, T. B. Marder and U. Radius, *Chem. Sci.*, 2022, **13**, 8321–8333.
44 W.-D. Li, Y. Wu, S.-J. Li, Y.-Q. Jiang, Y.-L. Li, Y. Lan and J.-B. Xia, *J. Am. Chem. Soc.*, 2022, **144**, 8551–8559.
45 Y. Liu, S. Lin, Y. Li, J.-H. Xue, Q. Li and H. Wang, *ACS Catal.*, 2023, **13**, 5096–5103.
46 C.-L. Wang, J. Wang, J.-K. Jin, B. Li, Y. L. Phang, F.-L. Zhang, T. Ye, H.-M. Xia, L.-W. Hui, J.-H. Su, Y. Fu and Y.-F. Wang, *Science*, 2023, **382**, 1056–1065.
47 C.-Z. Fang, B.-B. Zhang, Y.-L. Tu, Q. Liu, Z.-X. Wang and X.-Y. Chen, *J. Am. Chem. Soc.*, 2024, **146**, 26574–26584.
48 J. Koo, W. Kim, B. H. Jhun, S. Park, D. Song, Y. You and H. G. Lee, *J. Am. Chem. Soc.*, 2024, **146**, 22874–22880.
49 Z.-Q. Zhang, Y.-Q. Sang, C.-Q. Wang, P. Dai, X.-S. Xue, J. L. Piper, Z.-H. Peng, J.-A. Ma, F.-G. Zhang and J. Wu, *J. Am. Chem. Soc.*, 2022, **144**, 14288–14296.
50 Z. H. Zhang, M. J. Tilby and D. Leonori, *Nat. Synth.*, 2024, **3**, 1221–1230.
51 J. Corpas, M. Alonso and D. Leonori, *Chem. Sci.*, 2024, **15**, 19113–19118.
52 Z.-Q. Zhang, C.-Q. Wang, L.-J. Li, J. L. Piper, Z.-H. Peng, J.-A. Ma, F.-G. Zhang and J. Wu, *Chem. Sci.*, 2023, **14**, 11546–11553.
53 T. Wan, L. Capaldo, D. Ravelli, W. Vitullo, F. J. de Zwart, B. de Bruin and T. Noël, *J. Am. Chem. Soc.*, 2023, **145**, 991–999.
54 T. Wan, L. W. Ciszewski, D. Ravelli and L. Capaldo, *Org. Lett.*, 2024, **26**, 5839–5843.
55 X. Li, Y. Zhong, F. Tan, Y. Fei, X. Zhao, J. Xu and B. Fan, *Org. Chem. Front.*, 2025, **12**, 123–129.
56 S. Pillitteri, R. Walia, E. V. Van der Eycken and U. K. Sharma, *Chem. Sci.*, 2024, **15**, 8813–8819.
57 C.-L. Ji, J. Han, T. Li, C.-G. Zhao, C. Zhu and J. Xie, *Nat. Catal.*, 2022, **5**, 1098–1109.
58 L. Candish, M. Teders and F. Glorius, *J. Am. Chem. Soc.*, 2017, **139**, 7440–7443.
59 E. Speckmeier and T. C. Maier, *J. Am. Chem. Soc.*, 2022, **144**, 9997–10005.
60 L. Zhang and L. Jiao, *Chem. Sci.*, 2018, **9**, 2711–2722.
61 L. Zhang and L. Jiao, *J. Am. Chem. Soc.*, 2019, **141**, 9124–9128.
62 L. Bai and L. Jiao, *Chem*, 2023, **9**, 3245–3267.
63 B. Wang, P. Peng, W. Ma, Z. Liu, C. Huang, Y. Cao, P. Hu, X. Qi and Q. Lu, *J. Am. Chem. Soc.*, 2021, **143**, 12985–12991.